

Carbon Nanomaterial-Based Wing Temperature Control System for In-Flight Anti-Icing and De-Icing of Unmanned Aerial Vehicles

Kim Lynge Sørensen
 Norwegian University of
 Science and Technology
 O. S. Bragstads Plass 2D
 NO-7491, Trondheim, Norway
 kim.sorensen@itk.ntnu.no

Andreas Strand Helland
 AXTech
 Fannestrandvegen 85
 NO-6416 Molde, Norway
 ash@axtech.no

Tor Arne Johansen
 Norwegian University of
 Science and Technology
 O. S. Bragstads Plass 2D
 NO-7491, Trondheim, Norway
 tor.arne.johansen@itk.ntnu.no

Abstract—Structural changes due to ice accretion are common causes for unmanned aerial vehicle incidents in Arctic regions. For fixed wing unmanned aerial vehicles (UAVs) the leading edge of airfoil surfaces is one of the primary surfaces exposed to these changes, causing a significant reduction in aerodynamic ability, i.e. decreasing lift and manoeuvrability, and increasing drag, weight, and consequently power consumption. Managing or altogether preventing ice accretion could potentially prevent icing related UAV incidents and increase the operability of UAVs.

This paper addresses the issue of structural change, caused by ice accretion, on small UAVs by integrating a power control system and an electrically conductive carbon nano material based coating for temperature control of UAV airfoil surfaces. Performance assessment is achieved through extensive laboratory experiments, where various coating layouts have been investigated in various conditions, with temperatures ranging from +25° to -25°. The experimental setup consists of an Arduino microcontroller capable of controlling power delivery to the coating through feedback from thermocouples and a humidity sensor, sensing the surface temperature of the leading edge of the UAV wing and ambient humidity, respectively. Experiments reveal that a layout, where the coating covers the entire length of an wing is preferable, with the solution being highly capable of rapidly increasing the airfoil surface temperature (de-icing) when needed, and of maintaining an approximately constant airfoil surface temperature (anti-icing) when needed, all the while keeping power and energy consumption within weight and cost constraints imposed by the small scale of the UAV. The results represents a proof of concept by using an electrically conductive coating for de-icing and anti-icing of leading edge UAV airfoils.

TABLE OF CONTENTS

| | | |
|---|-------------------------------|---|
| 1 | INTRODUCTION | 1 |
| 2 | ICING & ICING CONDITIONS..... | 2 |
| 3 | ICE PROTECTION SYSTEM | 2 |
| 4 | THERMODYNAMICS | 4 |
| 5 | EXPERIMENTS | 4 |
| 6 | CONCLUSION | 5 |
| | ACKNOWLEDGMENTS | 6 |
| | REFERENCES | 6 |
| | BIOGRAPHY | 6 |

1. INTRODUCTION

The use of unmanned aerial vehicles (UAVs) has increased significantly within the last decade, primarily operating in

surveillance and reconnaissance. UAVs are very often suited for operating in conditions that are deemed unsafe for humans, Arctic operations being relevant and significant mentioning. Consequently, reliable, appropriate, and efficient UAV operation in a harsh environment, as the Arctic, is desirable.

In aviation, icing conditions are atmospheric conditions that can lead to the formation of ice on the surface of an aircraft, or within the aircraft's engine. In-flight icing can occur when an aircraft passes through air that contain droplets of water (humid air), and the temperature where the droplets impact with the aircraft is 0° C or colder. The impact of icing on an aircraft includes issues such as a reduction in lift and fuel efficiency, as well as an increase in drag, weight, and power requirements. Icing could be hazardous at every flight phase, particularly so for small scale UAVs operating at low altitudes. The effects of icing depends upon the location, and the type, of the formed ice. Icing can occur on wings, propellers, control surfaces, horizontal and vertical stabilizers, fuselage nose, landing gear doors, engine intakes, fuselage air data ports and sensors, and drain system outputs.

For manned aircraft, removing in-flight icing is ensured by manually activating an ice protection system. Most systems in use today can be categorized into two general types: thermal and pneumatic. Thermal systems melt the ice accretion or prevent the ice from forming by application of heat on the protected surface of the wing. This is done either through use of electric heaters or by ducting hot bleed air from engine. Pneumatic de-icing systems usually consist of an inflatable rubber boot located at the leading edge of the wing. This boot is inflated with air, causing the ice accreted over it to break and shed off the surface. Another alternative utilised is the use of chemicals that are applied to the aircraft surface prior to flight. The chemicals can be either dry or liquid, with shared feature of lowering the freezing point of water. The systems are usually heavy, expensive, and structurally intricate, and as such not applicable to small UAVs.

One solution could be the use of electrically conductive paints. These typically comprise copper or silver filled resins. However, such paints add weight due to the use of high density metal conductive fillers. In addition, such paints may also be subject to corrosion.

One alternative that could prove applicable to UAVs is found in [1] (a similar solution is found in [2]), where a heat conducting tape is bonded to the leading edge of an aircraft structure. The tape comprises a non-metallic electrical and heat-conducting layer consisting of flexible expanded graphite foil laminated to an outer heat-conducting layer. The solution

displays promising results, although power consumption is very high and no weight considerations are presented. In [3] laminated resistive heaters comprising a carbon nanotube (CNT) layer, is proposed. Several compositions are presented, where one includes a liquid carrier that facilitates the application of the composition to substrate surface, as an aircraft wing. Carbon nanomaterials have certain thermal and electrically conductive characteristics that make them exceedingly interesting as resistive heat sources [4]. Other relevant characteristics of carbon based nanomaterials are superior stiffness and strength, as well as their resistance to fatigue and corrosion [5].

The objective of the work presented in this paper is to introduce an ice protection system for small scale fixed-wing UAVs, where focus is on icing that forms on the leading edge of wings. The scope is to develop an inexpensive and lightweight solution comprised of off-the-shelf technologies and control engineering in a novel framework. As such the lightweight, off-the-shelf, easy-to-apply, and robust equipment due to weight restrictions of UAVs and harsh weather conditions, respectively, have been emphasized during the design phase.

The remainder of the paper is organized as follows. In Section 2 the environmental conditions leading to aircraft icing and the form it accumulates in, are presented. Section 3 is a presentation of the platform, hardware, and the ice protection system itself. Section 4 provides a review of the thermodynamic issues relevant for the ice protection system power consumption. In Section 5 a performance assessment of the ice protection system is presented. Finally, the paper is concluded in Section 6

2. ICING & ICING CONDITIONS

The following section presents an overview of the conditions leading to icing, to the different types of icing, and to the consequences these types of icing has on UAV operation.

For structural in-flight icing, as investigated in this paper, two conditions are necessary: (1) the aircraft must travel through visible water such as rain or cloud droplets, and (2) the temperature at the point where the moisture hits the aircraft must be 0°C or colder. Here it should be noted that aerodynamic cooling can decrease the temperature of an airfoil by a few degrees [6], [7].

Supercooled water increases the rate of icing and is essential to rapid accretion. Supercooled water is an unstable liquid state, where water is in a liquid form at temperatures well below 0°C. The phenomenon exists because the water lacks the ability to complete the nucleation process. At temperatures between 0°C and -25°C most clouds are composed of supercooled water droplets. When an aircraft is hit by a supercooled droplet of water, part of the droplet freezes instantaneously. The latent heat of fusion released by the freezing portion raises the temperature of the remaining portion to the melting point. Aerodynamic effects may cause the remaining portion to freeze. The way this remaining portion freezes determines the type of icing. The types of structural icing are clear, rime, and a mixture of the two. Each type has its identifying features.

• Clear ice

After moisture impacts the aircraft surface and after part of the droplet has frozen, clear ice forms as the remaining liquid

portion of the droplet flows out over the surface of the aircraft gradually freezing as a smooth sheet of solid ice. This type of icing usually forms when droplets are large as in rain or Cumuliform clouds. Clear ice is a hard and heavy type of ice.

• Rime

This type of icing occurs most frequently and are the consequence of stratified clouds or light drizzle. Rime ice is opaque and is caused by very small droplets of water, which after initial impact, freezes rapidly before the droplet can flow over the surface of the aircraft. Rime ice is lighter in weight than clear ice, so much so that for commercial aircraft the weight of this type of icing is negligible. For UAV's, however, which are usually small and light aircraft the weight of rime should be taken into consideration. Further, the irregular shape and rough surface of rime ice decreases the aerodynamic efficiency of the airfoil, thus increasing drag and reducing lift. Rime ice is considered to be brittle and is therefore removed more easily than clear ice.

• Mixed ice

Mixed ice forms when drops vary in size or when liquid drops are intermingled with snow or ice particles. It can form rapidly and forms as ice particles are embedded in clear ice. This builds a very rough accumulation on the leading edge of wings.

Potentially all clouds at subfreezing temperatures can cause icing. However, droplet size, distribution, and the aerodynamics of the aircraft all influence ice formation. Further, icing may not form even though the potential exists, as such the detection of ice accretion is another relevant and important research topic for UAV operations. On that topic the work conducted in [8] should be mentioned for its relevance considering model-based detection of UAV icing, and [5], where ice-detection is based upon the heat-capacity of a carbon nanotube layer located on the surface of the aircraft.

3. ICE PROTECTION SYSTEM

The main contribution of this paper is the ice protection system. This system is comprised of an electrically conductive coating that acts as a heat source when supplied with power, where each wing can be fitted with multiple zones of coating, depending on UAV platform. The power is supplied by a lithium-ion polymer (LIPO) battery. Feedback control is accomplished through a microcontroller receiving feedback from a thermocouple with amplifier, a transistor switch, and a humidity sensor.

UAV PLATFORM

For prototype purposes the X8 Skywalker UAV platform have been chosen to obtain the results presented in this paper.

The aircraft is a X-8 FPV wing from Skywalker Technology Co, Ltd. The fixed-wing UAV platform is moulded out of polystyrene, making it lightweight and durable. It has a wingspan of 2120 mm and is propelled by a rear mounted electrical engine delivering 400-800 Watt depending on payload. The thrust is delivered by an Aeronaut 13x8 folding propeller. Figure 1 displays the X8 UAV during operation.

Microcontroller

The Arduino Uno R3 is a microcontroller board based on the AVR 8-bit microcontroller ATmega328. The board has 14 digital input/output pins (of which 6 can be used as PWM outputs), 6 analog inputs, a 16 MHz ceramic resonator, a USB connection, a power jack, an ICSP header, and a reset button.



Figure 1. X-8 UAV from Skywalker Technology Co, Ltd.

Coating

The core of the ice protection system is a coating based on carbon nanomaterials graphene and carbon black, which is applied as a separate surface layer. The coating, acts as a mechanical reinforcement in addition to improving electrical conductivity considerably [4].

The coating, Carbo e-Therm PUR-120 1W, is an off-the-shelf product manufactured by FutureCarbon. The coating is a low-viscosity liquid and as such is easily applied. The electrical conductivity of the coating ($R < 1\Omega$ for typical layer thickness and size) enables rapid heat increase with low voltages (12/24V).

System Description

Each wing can be divided into multiple zones for purposes of energy efficiency and ease of application. A heating zone denotes a patch of coating where current is delivered using a bus bar system similar to what is presented in [2], [1]. A copper bus, measuring 5mm in width and 1mm in height, is embedded in the coating, by gluing it to the surface of the wing and applying the coating on top of it, at two opposing edges of a zone.

The standalone ice protection system presented here consists of six components: (1) resistivity of the coating, (2) a temperature sensor, providing the microcontroller with on-line measurements of coating temperature, (3) a humidity sensor, supplying the microcontroller with on-line measurements of ambient relative humidity, (4) a transistor (N-channel MOSFET), receiving a PWM signal from the microcontroller, is used to regulate the power supplied to the coating, (5) a power supply, where a LIPO battery has been chosen for its high power and low weight characteristics, and finally (6) a micro controller in the form of an Arduino Uno R3. The system also includes a pull-down resistor (per zone) of $10k\Omega$. A schematic outlining the set-up, is seen in Figure 2.

The system is easily expanded to include more zones by inserting a thermocouple and transistor for each new required coating zone. Each micro controller can manage four zones.

The temperature of each zone is controlled by the microcontroller utilising a standard proportional-integral-derivative (PID) controller and feedback from a temperature measurement of the coating temperature and a measurement of the relative humidity of the surrounding environment. Input to the PID is the temperature measurement alone, as the humid-

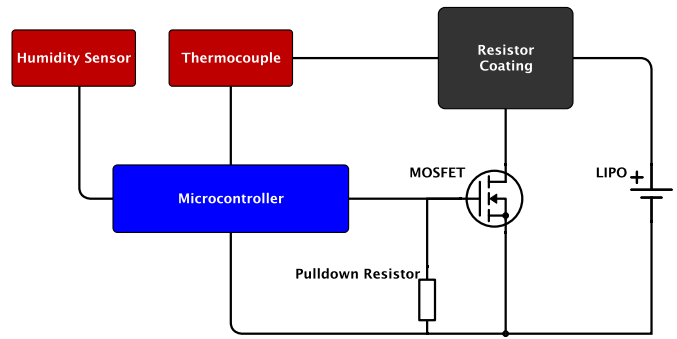


Figure 2. Schematic of ice protection system.

ity measurement is used as an on/off switch only. Output of the PID comes in the form of integer values ranging from 0 to 255, where 0 signifies a disconnect between the MOSFET drain and source, and 255 signifies complete connection.

The temperature sensor used is of the type thermocouple type-K glass braid insulated from Adafruit and the humidity sensor is a Honeywell HIH-4000 series.

Functionality

The primary objective of any UAV ice protection system is to allow for UAV operations regardless of any atmospheric conditions. This motivates two different ice protection routines, (1) an anti-icing routine, and (2) a de-icing routine. The former will be useful for UAV operations in approximately constant potential icing condition, and the later when potential icing conditions could occur in periods. For both routines the humidity sensor acts as a threshold-based on/off switch.

Below is a brief description of how the anti-icing routine operate and an outline of the de-icing routine.

• Anti-Icing Routine

When the ice protection operates at this routine, atmospheric conditions are approximately constant potential icing conditions, i.e. high humidity and subzero ambient temperatures. Here the control objective is to keep a constant positive set-point temperature (degrees Celsius) of the coating. This objective is achieved by gradually supplying power to the coating through the MOSFET, which is activated by a PWM signal from the microcontroller. When set-point is reached, power to the coating is stopped as connection through the MOSFET is disrupted. The routine will keep the temperature of the coating approximately constant until ambient temperature rises beyond the set-point, or the humidity falls below threshold.

• De-Icing Routine

The de-icing routine is intended for changeable and potential icing conditions that occur only in periods. For these operating conditions the control objective is to rapidly heat the coating to any temperature that will cause the bonding icing layer to reach melting point, consequently shedding the ice. This can be achieved by an initial ice detection based on heat-capacity, where a step function of power is applied to the coating for very brief periods (seconds), and a temperature rise can be recorded. The slope of the rise can be well correlated to the ice thickness [5]. Another detection approach is model-based, where the accumulation of ice is detected as a structural fault, i.e. an unexpected degradation of aerodynamic capabilities as presented in [8].

During both routines the coating temperature should ensure an ice free surface. The melting point of ice is approximately 0° at all relevant operational altitudes, but as airspeed and aerodynamics further decrease surface temperature, temperature levels of the coating should exceed 0° .

4. THERMODYNAMICS

When the potential of icing is zero, the coating, the coating-covered parts of the wing, and the surrounding air forms a thermodynamic system in equilibrium, i.e. their temperatures are equal. But when icing conditions are present the coating is heated, consequently the thermodynamic system is driven out of equilibrium and energy starts to flow, as heat flows from the coating to the wing and to the surrounding air. The heat flow from the coating to the wing is known as conduction. The law of heat conduction also known as Fourier's law is mathematically given in its integral form as

$$\frac{\partial Q}{\partial t} = -k \oint_S \vec{\nabla} T \cdot d\vec{A}, \quad (1)$$

where $\partial Q/\partial t$ is the rate of heat per unit time and k is the thermal conductivity of the wing material, i.e. a measure of the materials ability to transfer heat. ∇T is the temperature gradient and dA is the surface element. When integrating (1) the heat flow rate becomes

$$\frac{\Delta Q}{\Delta t} = -kA \frac{\Delta T}{\Delta x}, \quad (2)$$

where, for the specific case presented in this paper, ΔT is the temperature difference between the coating and the opposite coating-free side of the wing. Δx is the thickness of the wing.

The flow of heat from the coating to the surrounding air is in thermodynamics called convection. Convective heat transfer is complicated since it involves fluid motion as well as heat conduction. The fluid motion enhances heat transfer (the higher the velocity the higher the heat transfer rate). One mathematical expression, attributed to Newton, that describes heat convection is given by

$$\frac{dQ}{dt} = -hA(T - T_0), \quad (3)$$

that is the rate of heat loss dQ/dt of a body at temperature T surrounded by a fluid or gas at temperature T_0 is proportional to the difference $(T - T_0)$ and the body's surface area A . h is the convective heat transfer coefficient, which depends on the type of media, gas or liquid, the flow properties such as velocity, viscosity, and other flow and temperature dependent properties.

The complexities of fluid flow make it a highly intricate task to develop an analytical expression for h , consequently so for convection itself. Therefore, most relationships in convection are based on experimental correlations [9], [10].

5. EXPERIMENTS

Initial Experiments

Each zone is coated using a paint-gun. Several layers are applied to a zone ensuring some degree of uniformity as seen in Figure 3, which was captured by a thermal camera. An appropriate layer thickness is 0.04mm to 0.06mm [11].

Note that the zone layout here is a combination of two zones activated simultaneously, each measuring 5cm by 25cm. The ambient temperature during this test was 24°C , 12V was supplied and the measured temperature was 62.6°C .

Further, as an initial investigation into the performance of the coating a max test was conducted on a zone measuring 10cm by 10cm. Ambient temperature was measured to be 28.4°C . With 12V, applied the temperature of the zone increased by more than 100°C in 11 seconds, with an instant power consumption of approximately 100W.

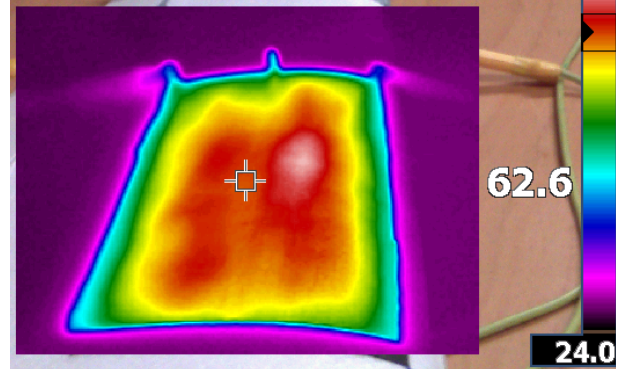


Figure 3. Thermal camera capturing uniformity test on coated zone measuring two times 5cm by 25cm, with 12V supplied.

Due to the high level of uniformity, relatively small scale of the UAV, with each wing area measuring 0.8m^2 , and for ease of integration, a suitable zone size was chosen to be 8cm by 75cm. Figure 4 display the applied layout.



Figure 4. X8 wing with two coating zones.

This configuration (seen in Figure 4) increases the weight of the wing by approximately 100g, 50g for each zone including temperature sensors and cables. The controller and all the components regarding coating temperature control, which also includes a data logging shield and LIPO battery, has a total weight of approximately 300g. The utilised platform has enabled thermocouple integration through the wing, i.e. the sensor is embedded in the wing with only the sensory part protruding the surface of the wing.

Controller Response

Experiments were conducted in an icing chamber where the environment temperature is controllable, but where humidity is not, consequently during experiments in this chamber, humidity level is assumed to be above threshold, nor was ice or water part of these experiments.

The experiments were conducted with one active zone for a proof-of-concept. Energy supply to the zone was limited to

2V for the coating with an internal resistance of 0.5Ω , for a maximum of 8W supplied to the coating. Limiting the power supply is a trade-off between instant performance and operational duration, as well as a consideration regarding a multiple zones integration. Operating at voltages this low the MOSFET drain to source current is assumed to evolve approximately linearly. The PID controller has a rise time of approximately 13 seconds.

A test of the system was conducted by applying temperature set-point T_d steps. The system was in an approximately thermal equilibrium at -13°C , which for simplicity is chosen as time $t = 0$. Initially the temperature set-point was at $T_d = -15^\circ\text{C}$. The first step was introduced at $t = 20$ seconds, with $T_d = -10^\circ\text{C}$, second step was at $t = 200$, with $T_d = -5^\circ\text{C}$, and the final step was introduced at $t = 400$ seconds, for $T_d = 0^\circ\text{C}$. A visual representation of the test is found in Figure 5, where T_m is the measured temperature and T_d , as mentioned, is the desired set-point temperature. Note that the rugged edges of the temperature changes are attributed to the sensitivity of the thermocouple of approximately 0.25°C . An explanation of the response is provided in the following.

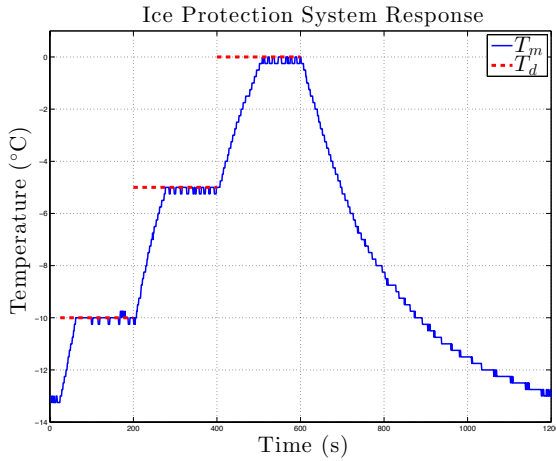


Figure 5. Ice protection system temperature response to changes in set-point temperature.

- The first step indicates a set-point increase to -10°C , as the system is at thermal equilibrium at -13°C , the temperature increase required by the system is of 3°C . The new set-point is reached after 62 seconds. The system is kept in a thermal non-equilibrium at -10°C by the PID controller balancing the power supplied to the coating. While the temperature is kept at a given set-point, power is not supplied constantly, it is only when the temperature drops below the set-point that power is again supplied.
- At the second step a requirement of a temperature increase from -10°C to -5°C is imposed upon the system. The new set-point is reached after 77 seconds.
- The final step takes the set-point from -5°C to 0°C , which is reached after 109 seconds. The difference in settling times of step two and three are attributed to an increase in thermal convection, as the temperature difference between ambient and coating have doubled.

The heat transfer, experienced during the described experiment, has been estimated utilising the thermodynamic theory presented in Section 4 based on a heat conductivity value of 0.0244 W/mK and an average heat transfer coefficient of approximately $0.1362 \text{ W/m}^2\text{K}$ [9]. Note that the latter is

highly dependant on airspeed, and as such will increase by a factor of approximately 200, for an airspeed of 20 m/s leading to a dramatic increase in convective thermal transfer [9].

Figure 6 display the heat transfer response to the changes in set-point temperature, where the conduction is the heat transfer with the wing and convection is heat transfer with the air. The two combined is also displayed in the aforementioned figure.

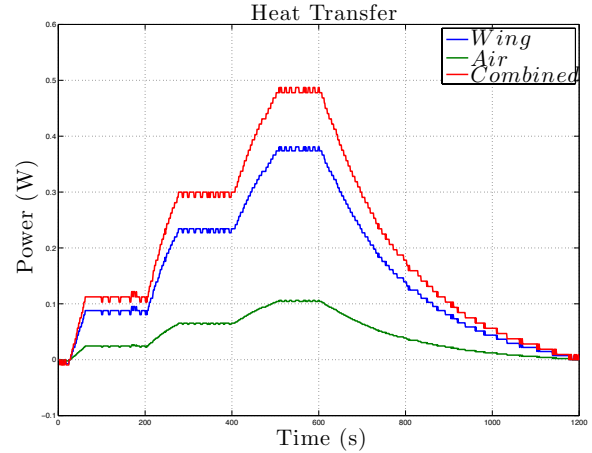


Figure 6. Thermal conduction and convection during temperature step experiment.

6. CONCLUSION

Maximising operational output while maintaining integrity of UAVs operating in regions with potential icing conditions is essential to further advance use of UAVs for high risk operations, thereby reducing any human incidents and decreasing operational cost.

The work presented in this paper proposes an ice protection system based on an electrically conductive carbon nanomaterial coating, and a power management system, for thermal control of relevant UAV aircraft surfaces, where focus of the work in this paper has been on the leading edge of fixed wing UAVs.

Realisation of the system has, through experiments, demonstrated several important aspects of its feasibility. The coating has displayed electrically conductive characteristics suitable for a resistive heat source applied for thermal control of potential icing exposed UAV surface areas, as both uniformity and maximum temperature investigations displayed adequate responses. The low internal resistivity of the coating allow for the usage of low voltages, enabling the use of a low-weight power source in the form of LIPO batteries. A microcontroller was programmed with a PID controller, receiving feedback from a thermocouple, and utilised as control unit, managing the power supplied to the coating, through a transistor switch.

Experiments confirm the expected performance of the system: despite thermal conduction and convection temperature of the coating is promptly and successfully regulated to its desired set-point value. Further, the control objective was fulfilled with a control effort well within the capabilities of the system.

ACKNOWLEDGMENTS

This work has been carried out at the Centre for Autonomous Marine Operations and Systems (AMOS), supported by the Research Council of Norway through the Centres of Excellence funding scheme, Project number 223254 - AMOS. The Norwegian Research Council is acknowledged as the main sponsor of AMOS.

Deep gratitude needs to be expressed to Philip A. McGilivray, science liaison to the US coast guard, for sharing his experiences, ideas, and resources.

Acknowledgement should also go to Professor Alex Klein-Paste working out of the department of Civil and Transport Engineering, Norwegian University of Science and Technology, for his sincerest interest in the work conducted, and for allowing the use of the departments temperature chamber.

REFERENCES

- [1] R. Rutherford and R. Dudman, "Zoned aircraft de-icing system and method," may 2001, uS Patent 6,237,874. [Online]. Available: <http://www.google.com/patents/US6237874>
- [2] O. H. Hastings and O. M. Hastings, "Electrically conductive laminate for temperature control of aircraft surface," sep 2004, uS Patent 5,344,696. [Online]. Available: <https://www.google.com/patents/US6194685>
- [3] A. Heintz, K. Mitchell, B. Burton, I. Feier, T. Lastrapes, and B. Muszynski, "Carbon nanotube thin film laminate resistive heater," February 2014, uS Patent App. 13/988,037. [Online]. Available: <http://www.google.com/patents/US20140034633>
- [4] Z. Han and A. Fina, "Thermal conductivity of carbon nanotubes and their polymer nanocomposites: A review," *Progress in Polymer Science*, vol. 36, no. 7, pp. 914 – 944, 2011, special Issue on Composites. [Online]. Available: <http://www.sciencedirect.com/science/article/pii/S0079670010001243>
- [5] S. S. Wicks, R. G. de Villoria, B. L. Wardle, S. S. Kessler, and C. T. Dunn, "Carbon nanotube (cnt) enhancements for aerosurface state awareness," in *Proceedings of the Workshop on Structural Health Monitoring, 2011 8th annual IWSHM*, September 2011.
- [6] G. Mingione, M. Barocco, E. Denti, and F. G. Bindi, "Flight in icing conditions," *Direction gnrale de l'aviation civile, DGAC, Tech. Rep.*, 1997.
- [7] W. J. White, "Effect of icing on aircraft cotnrol, and airplane de-icing and anti-icing systems," U.S. Department of Transportation, Federal Aviation Administration, Tech. Rep., 1996.
- [8] M. Tousi and K. Khorasani, "Fault diagnosis and recovery from structural failures (icing) in unmanned aerial vehicles," in *Systems Conference, 2009 3rd Annual IEEE*, March 2009, pp. 302–307.
- [9] C. P. Kothandaraman, *Fundamentals of Heat and Mass Transfer*, 3rd ed. New Age International Limited, Publishers, 2006.
- [10] J. Welty, C. Wicks, G. Rorrer, and R. Wilson, *Fundamentals of Momentum, Heat, and Mass Transfer*, 5th ed. John Wiley and Sons Limited, 2007.
- [11] FutureCarbon, "carbo-e-therm," <http://www.future-carbon.de/solutions/electrical-heating/carbo-e-therm/>, 2014.

- [12] J. J. Ballough, "Advisory circular, pilot guide: Flight in icing conditions," U.S. Department of Transportation, Federal Aviation Administration, Tech. Rep., 2007.
- [13] R. A. Siquig, "Impact of icing on unmanned aerial vehicle (uav) operations," Naval Oceanographic and Atmospheric Research Laboratory, Tech. Rep., 1990.
- [14] M. K. Politovich, "Aircraft icing," National Center for Atmospheric Research, Tech. Rep., 2003.
- [15] R. W. Beard and T. W. McLain, *Small Unmanned Aircraft - Theory and Practice*. Princeton University Press, 2012.
- [16] E. O. Ogretim, W. W. Huebsch, J. Narramore, and B. Mullins, "Investigation of relative humidity and induced-vortex effects on aircraft icing," *Journal of Aircraft*, vol. 44, no. 6, pp. 1805–1814, November-December 2007.
- [17] D. Kondepudi, *Introduction to Modern Thermodynamics*. John Wiley and Sons Limited, 2008.

BIOGRAPHY



Kim Lyng Sørensen received his B.Sc. and M.Sc. degrees in electrical engineering, specialising in robot technology, from the Technical University of Denmark in 2011 and 2013, respectively. In 2013 he began his PhD when he became a member of the centre for Autonomous Marine Operations and Systems, Department of Engineering Cybernetics, at the Norwegian University of Science and Technology, where his current research primarily revolves around icing on UAVs.



Andreas Strand Helland received his M.Sc. degree in engineering cybernetics from the Norwegian University of Science and Technology in 2014. Currently he is a member of the technical staff at Norwegian based AXTech Marine and Offshore Lifting Equipment.



Tor Arne Johansen received his M.Sc. degree in 1989 and Ph.D. degree in 1994, both in electrical and computer engineering from the Norwegian University of Science and Technology. He worked at SINTEF Electronics and Cybernetics as a researcher before he was appointed Associated Professor in Engineering Cybernetics at the Norwegian University of Science and Technology in 1997 and was promoted to Professor in 2001. In December 2002 Prof. Johansen co-founded the company Marine Cybernetics AS, where he was Vice President until 2008. Prof. Johansen received the 2006 Arch T. Colwell Merit Award of the SAE. He is currently a key member of the scientific staff at the centre for Autonomous Marine Operations and Systems, at the Norwegian University of Science and Technology.